Title

Adipocyte SIRT1 knockout promotes PPARγ activity, adipogenesis and insulin sensitivity in chronic-HFD and obesity

Journal

Molecular Metabolism, 4(5)

ISSN

2212-8778

Authors

Mayoral, Rafael

Osborn, Olivia

McNelis, Joanne

et al.

Publication Date

2015-05-01

DOI

10.1016/j.molmet.2015.02.007

Peer reviewed

Original article

MOLECULAR METABOLISM

Adipocyte SIRT1 knockout promotes PPARγ activity, adipogenesis and insulin sensitivity in chronic-HFD and obesity

Rafael Mayoral [1,2], Olivia Osborn [1], Joanne McNelis [1], Andrew M. Johnson [1], Da Young Oh [1], Cristina Llorente Izquierdo [3], Heekyung Chung [1], Pingping Li [1], Paqui G. Traves [4], Gautam Bandyopadhyay [1], Ariane R. Pessentheiner [5], Jachelle M. Ofrecio [1], Joshua R. Cook [6], Li Qiang [6], Domenico Accili [6], Jerrold M. Olefsky [1,*]

ABSTRACT

Objective: Adipose tissue is the primary site for lipid deposition that protects the organisms in cases of nutrient excess during obesogenic diets. The histone deacetylase Sirtuin 1 (SIRT1) inhibits adipocyte differentiation by targeting the transcription factor peroxisome proliferator activated-receptor gamma (PPARγ).

Methods: To assess the specific role of SIRT1 in adipocytes, we generated *Sirt1* adipocyte-specific knockout mice (ATKO) driven by aP2 promoter onto C57BL/6 background. *Sirt1*$^{flx/flx}$ *aP2Cre*$^{+}$ (ATKO) and *Sirt1*$^{flx/flx}$ *aP2Cre*$^{-}$ (WT) mice were fed high-fat diet for 5 weeks (short-term) or 15 weeks (chronic-term). Metabolic studies were combined with gene expression analysis and phosphorylation/acetylation patterns in adipose tissue.

Results: On standard chow, ATKO mice exhibit low-grade chronic inflammation in adipose tissue, along with glucose intolerance and insulin resistance compared with control fed mice. On short-term HFD, ATKO mice become more glucose intolerant, hyperinsulinemic, insulin resistant and display increased inflammation. During chronic HFD, WT mice developed a metabolic dysfunction, higher than ATKO mice, and thereby, knockout mice are more glucose tolerant, insulin sensitive and less inflamed relative to control mice. SIRT1 attenuates adipogenesis through PPARγ repressive acetylation and, in the ATKO mice adipocyte PPARγ was hyperacetylated. This high acetylation was associated with a decrease in Ser273-PPARγ phosphorylation. Dephosphorylated PPARγ is constitutively active and results in higher expression of genes associated with increased insulin sensitivity.

Conclusion: Together, these data establish that SIRT1 downregulation in adipose tissue plays a previously unknown role in long-term inflammation resolution mediated by PPARγ activation. Therefore, in the context of obesity, the development of new therapeutics that activate PPARγ by targeting SIRT1 may provide novel approaches to the treatment of T2DM.

Keywords Obesity; SIRT1; PPAR03B3; Glucose homeostasis; Insulin resistance; Phosphorylation

1. INTRODUCTION

Obesity is a complex metabolic disorder associated with insulin resistance, glucose intolerance and hepatic steatosis. In this syndrome, the white adipose tissue plays an important role as the primary storage site for lipid deposition. Increased caloric intake causes an expansion of adipocyte size, with subsequent activation of stress pathways, leading to metabolic deterioration and decreased insulin sensitivity. This process is associated with increased infiltration of inflammatory cells into the adipose tissue, which contribute to the development of insulin resistance [1,2].

Sirtuin 1 (SIRT1, one of the seven mammalian sirtuins) is the ortholog of the yeast protein Silent information regulator 2 (Sir2) and a nuclear NAD^{+}-dependent class III histone deacetylase class III which engages in reciprocal co-regulation of many different binding partners [3,4]. SIRT1 is regulated by cellular NAD^{+} levels and several studies have shown that its expression and activity increases during fasting or calorie restriction whereas decreases by over nutrition in rodents and humans [3,5,6]. Thus, SIRT1 couples host metabolic status to gene expression regulation through deacetylation of histones, transcription factors, and transcriptional co-regulators. In this way, SIRT1 controls metabolic homeostasis via the integration of diverse actions across different tissues, including brain, liver, pancreas and adipose tissue [3,7].

[1]Division of Endocrinology and Metabolism, Department of Medicine, University of California San Diego (UCSD), La Jolla, CA 92093, USA [2]Networked Biomedical Research Center, Hepatic and Digestive Diseases (CIBERehd), Monforte de Lemos 3-5, ISC-III, 28029 Madrid, Spain [3]Division of Gastroenterology, Department of Medicine, University of California San Diego (UCSD), La Jolla, CA 92093, USA [4]Molecular Neurobiology Laboratory, The Salk Institute, La Jolla, CA 92037, USA [5]Institute of Biochemistry, Humboldtstrasse 46/3, 8010 Graz, Austria [6]Naomi Berrie Diabetes Center, Department of Medicine, Columbia University, New York, NY 10032, USA

*Corresponding author. Division of Endocrinology & Metabolism, Department of Medicine, UCSD, 9500 Gilman Drive, La Jolla, CA, 92093, USA. Tel.: +1 858 534 6651; fax: +1 858 534 6653. E-mail: jolefsky@ucsd.edu (J.M. Olefsky).

Received February 14, 2015 • Revision received February 20, 2015 • Accepted February 24, 2015 • Available online 5 March 2015

http://dx.doi.org/10.1016/j.molmet.2015.02.007

In adipose tissue, SIRT1 controls lipolysis and inhibits inflammation by repressing PPARγ and NFκB activity [8,9]. Furthermore, SIRT1 expression is inversely correlated with macrophage infiltration in subcutaneous fat from obese humans [10]. Thus, activation of SIRT1 has been proposed as a therapeutic target for the treatment of obesity and associated metabolic disorders [11,12]. However, this proposition is contradictory to the proven benefits of enhancing PPARγ activity in obese/diabetic individuals [13], and inhibition of PPARγ activity in insulin resistant subjects requires careful study.

In the current work, we sought to better understand the physiological role of adipocyte SIRT1 with the aim of resolving this contradiction and clarifying its therapeutic potential by generating an adipocyte-specific knockout mouse (ATKO). We report clear evidence that selective adipocyte deletion of SIRT1 exacerbates the detrimental effects of acute HFD-feeding. Strikingly, we find protective effects of SIRT1-deletion in the context of chronic HFD exposure. These beneficial outcomes of SIRT1-deletion were associated with increased PPARγ activity resulting from hyperacetylation and dephosphorylation of PPARγ Ser273 along with reduced CDK5 activity. Thus we propose that, in the context of chronic HFD/obesity, inhibition of SIRT1 in adipocytes can result in improved metabolic functions.

2. MATERIALS AND METHODS

2.1. Animals

We backcrossed mice carrying *Sirt1* floxed alleles (fl/fl mice) [14] onto C57BL/6 background for more than 6 generations. Mice were bred with transgenic mice harboring Cre recombinase driven by aP2 promoter [15,16] to create the following genotypes: WT (*Sirt1*$^{flx/flx}$ *aP2Cre*$^{-}$) or ATKO (*Sirt1*$^{flx/flx}$ *aP2Cre*$^{+}$). Mice were housed on a 12-h light/dark cycle and given ad libitum access to food and water. Mice were fed either with NC (13.5% fat; LabDiet) or HFD (60% fat; D12492, Research Diets) starting at 8 weeks of age. All protocols were approved by the Animal Subjects Committee of the University of California, San Diego.

2.2. Adipocytes, stromal vascular fraction, and peritoneal macrophages isolation

Adipocytes and SVFs were prepared from collagenase-digested adipose tissue, as described previously [16]. Peritoneal macrophages were prepared from WT and ATKO mice as previously described [17].

2.3. RNA isolation and real-time PCR

Total RNA was isolated with TRIzol reagent (Invitrogen) and cDNA was synthesized with Transcriptor First Strand cDNA Synthesis Kit (Roche Applied Science). Semi-quantitative PCR was performed with MyTaq DNA Polymerase (Bioline) and quantitative real-time PCR (qPCR) with iTaq SYBRgreen Supermix (BioRad). We calculated relative gene expression levels by ΔΔCt method using *36b4* (*Rplp0*) as internal control. Expression of genes regulated by the phosphorylation of PPARγ was described before by Choi et al. [18]. Primers are summarized in Table S1.

2.4. Western blot analysis

Proteins from total tissue lysates were prepared as previously described [19], separated by SDS-PAGE and probed with different primary antibodies against Sirt1, Anti-phospho-Akt (Ser473), total Akt, PPARγ, phospho-CDK5 (Tyr15), CDK5, and Hsp90α/β (Santa Cruz); Acetyl (Lys379) p53, p53 and NF-κB p65 (Cell Signalling); Acetyl (Lys310) NF-κB p65 and FGF21 (Abcam); Anti-phospho- PPARγ (Ser 273) was a kind gift from Dr. Bruce Spiegelman. For immunoprecipitation (IP), eWAT was homogenized in IP Lysis/Wash Buffer and 500 μg of total protein were incubated with the antibody-conjugated magnetic cross-linked beads for 1 h at RT. The immuneprecipitates were eluted according to the manufacturer's instructions (Thermo Scientific). In order to avoid interferences with denatured rabbit IgG heavy chains, we used a mouse anti-rabbit IgG conformation specific as a secondary antibody (L27A9, Cell Signaling). The antibody-conjugated magnetic beads were prepared with 5 μg of PPARγ (H100) (Santa Cruz). Blots were visualized using a CCD camera in a Molecular Imaging System (ChemiDoc XRS+, Bio-Rad).

2.5. Metabolic studies

Glucose and insulin tolerance tests were performed on mice fasted for 6 h by intraperitoneal injection of 1 g/kg dextrose (Hospira) or 0.6 U/kg insulin (Novolin R, Novo-Nordisk) respectively. Blood glucose concentrations were measured at 0, 15, 30, 60, 90 and 120 min after dextrose or insulin injection. Plasma levels of Insulin were measured by ELISA (ALPCO). Hyperinsulinemic-euglycemic clamps were performed after 6 h of fasting using a method described previously [20]. Plasma FFA levels were measured enzymatically (WAKO Chemicals). Acute insulin challenge experiments were performed on anesthetized mice fasted for 6 h. Basal samples of liver, muscle, and fat were taken and vessels were ligated. Five minutes after injection via inferior vena cava with 0.6 U/kg of insulin, the remaining liver, muscle, and fat were snap frozen for subsequent protein extraction. Glucose uptake in eWAT explants was performed as previously described [21].

2.6. Confocal microscopy and determination of adipocyte cell size

The method for immunofluorescene study of mouse adipose tissue was followed as described [22]. Adipocyte area was measured from each section using Image Gauge v4.0 software (Fujifilm). Frequency, histograms and Gaussian distributions were calculated using Excel 2013 (Microsoft) and GraphPad Prism v6.0 (GraphPad Software).

2.7. Statistical analysis

Results are presented as the mean ± SEM. Statistical significance was determined using GraphPad Prism v6.0 (GraphPad Software) or Excel 2013 (Microsoft) at $P < 0.05$. Student t-test was used to compare differences between two groups. Two-way ANOVA and Bonferroni posttest were used to analyze multiple experimental groups.

3. RESULTS

3.1. Adipocyte-specific *Sirt1* knockout mice (ATKO)

In order to investigate the specific role of adipocyte SIRT1 on the development of insulin resistance, we generated an adipocyte-specific knockout mouse (ATKO) using the Cre-lox system. We bred mice carrying the floxed *Sirt1* allele, containing two loxP sites flanking exon 4, which encodes the deacetylase domain, to transgenic mice expressing Cre recombinase driven by the *aP2* promoter [10,14,15]. In this model, restricted Cre expression in both white and brown adipose tissue results in a smaller SIRT1 protein with an intact C terminus but without deacetylase activity [23].

Floxed *Sirt1* and *Cre* genotypes were determined from genomic DNA (Figure 1A), and the generated genotypes were denominated WT (*Sirt1*$^{fl/fl}$ *aP2Cre*$^{-}$) or ATKO (*Sirt1*$^{fl/fl}$ *aP2Cre*$^{+}$). Growth and fertility between ATKO mice and their control littermates were comparable. We verified by PCR from DNA that the excision of exon 4 occurs only in fat tissues and is restricted to adipocytes. We have found no-Cre mediated target gene recombination in liver, spleen, kidney, muscle or peritoneal macrophages (Δ4 ATKO, Figure 1B,C). The exon 4 deletion was predominantly detected in mature adipocytes and not in cells from the

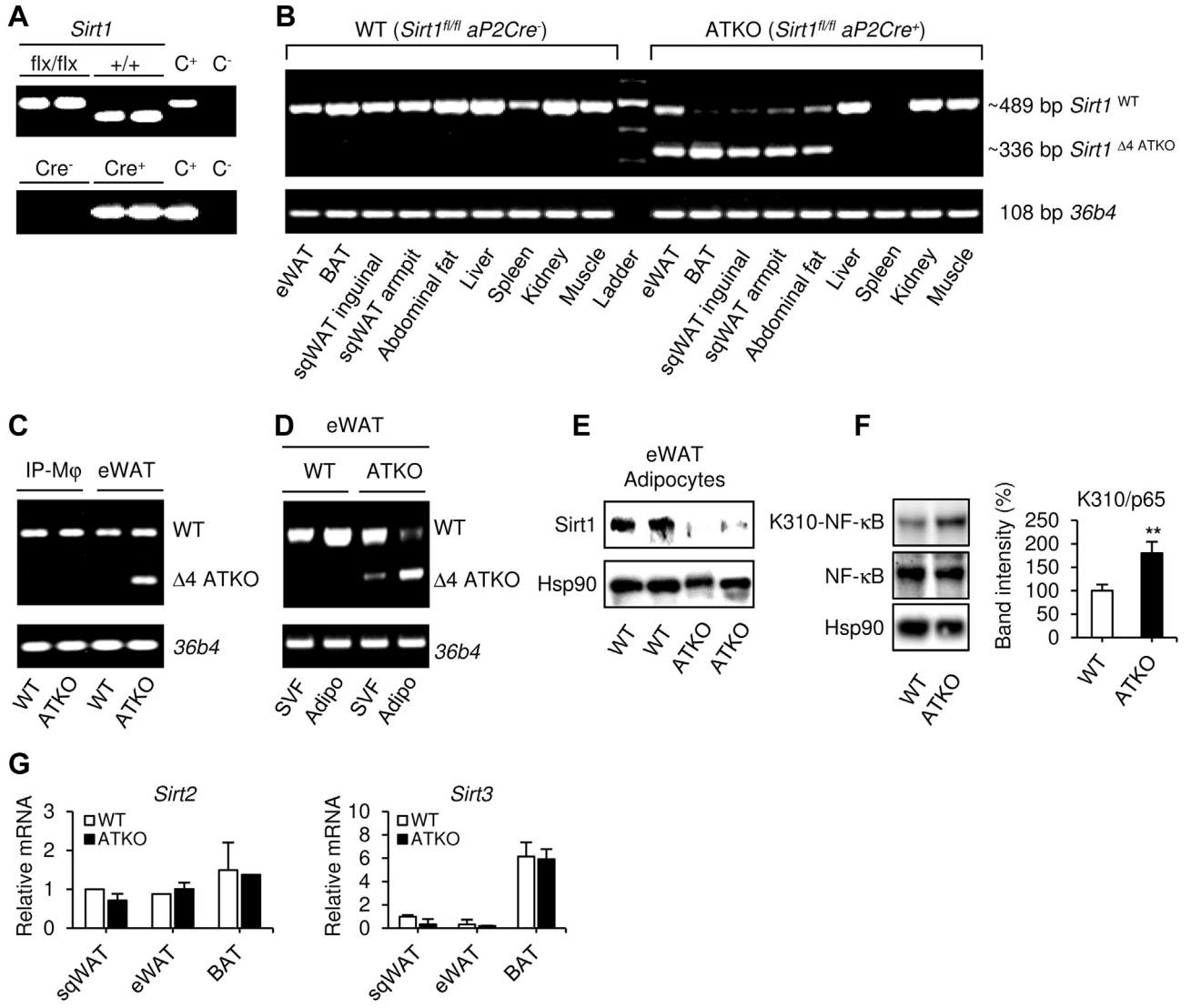

Figure 1: Quantification of adipocyte-specific deletion of *Sirt1* in mice (ATKO). **A**: DNA genotyping. Upper panel, *Sirt1*$^{flx/flx}$ (floxed-ATKO) and *Sirt1*$^{+/+}$ (WT) DNA expression. Lower panel, *Cre*-Recombinase (all mice are *Sirt1*$^{flx/flx}$). C+, Cre positive control; C- Cre negative control. **B**: Semi-qPCR showing the *Sirt1* floxed exon 4 (Δ4 ATKO) in several adipose depots and other different tissues from WT and ATKO mice. *36b4* (*Rplp0*) expression was used as housekeeping gene. **C**: *Sirt1* mRNA expression in intraperitoneal macrophages and epididymal white adipose tissue (eWAT). **D**: Semi-qPCR showing *Sirt1* mRNA expression in adipocytes or Stromal vascular fraction (SVF) from WT and ATKO eWAT. **E**: Protein expression of SIRT1 determined by Western Blot in adipocytes isolated from eWAT. **F**: Acetylation levels of SIRT1 target protein p65 (NF-κB) in adipocytes from ATKO or WT mice. Hsp90 expression was used as loading control. The Western blots shown are representative of three independent experiments (**P $\leq$ 0.01 vs. WT). **G**: Relative mRNA expression of *Sirt2* and *Sirt3* in different adipose tissues from WT and ATKO mice after 15 weeks of HFD.

stromal vascular fraction (SVF) (Figure 1D,E). To confirm the magnitude of the SIRT1 deacetylase site deletion, we measured the acetylation status of NF-κB, one well-known SIRT1 target. In adipocytes, increased p65 acetylation was detected in ATKO mice (Figure 1F). In addition, WT and ATKO mice did not show any differences in gene expression levels of *Sirt2* and *Sirt3* in white and brown adipose tissues (Figure 1G).

3.2. Adipocyte *Sirt1* deletion causes insulin resistance on chow diet

Due to the described role of SIRT1 as an inhibitor of inflammatory pathways and modulator of insulin sensitivity in macrophages and adipocytes [9,24], we analyzed the metabolic phenotype of mice with adipocyte specific deletion of *Sirt1*. Initially the body weights of ATKO and WT mice fed NCD were comparable until 23 weeks of age after which the ATKO mice gained significantly more weight than WT controls (Figure 2A). At 15 weeks of age, we harvested fat depots from WT and ATKO mice fed NCD and found that ATKO mice showed increased subcutaneous, epididymal, and brown adipose tissue (Figure 2B). Before the divergence in body weight (Figure 2C), we conducted glucose tolerance and insulin tolerance tests. ATKO mice at 19 weeks of age were hyperinsulinemic, with impaired glucose and insulin intolerance compared to WT mice (Figure 2D,E and F). Indeed, elevated basal insulin levels could be detected in ATKO mice as soon as 8 weeks of age although no differences in glucose tolerance were observed at this age (Figure 2D,E). We also measured insulin-stimulated glucose uptake in primary adipocytes, and we confirmed that the ability of insulin to enhance glucose transport was reduced in ATKO versus WT mice (Figure 2G).

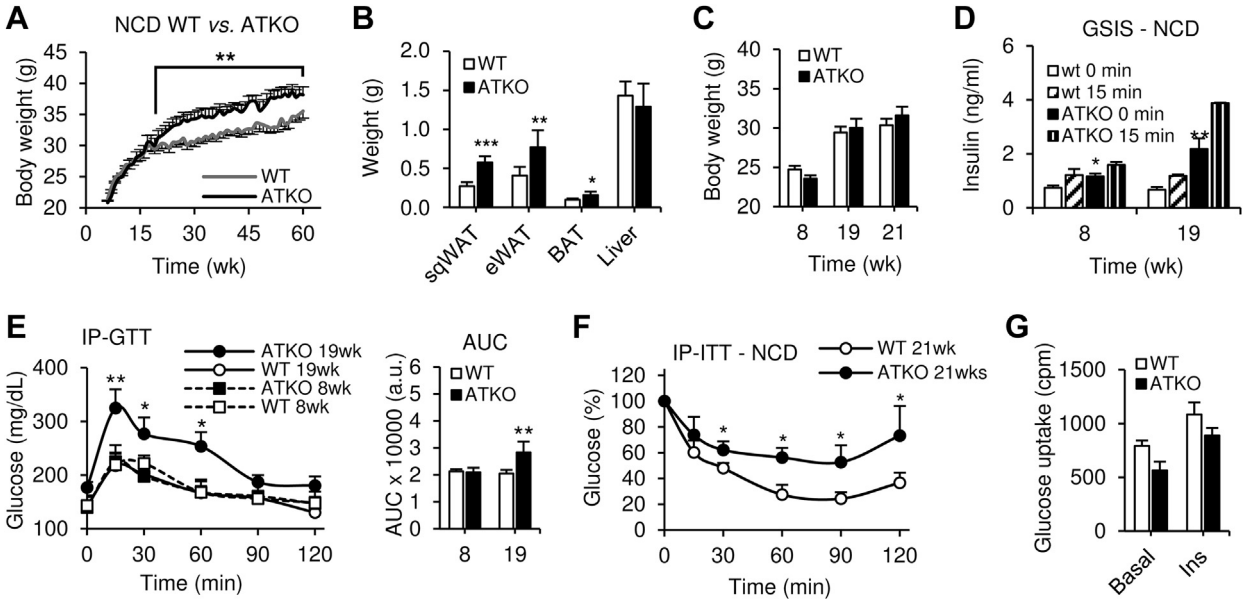

Figure 2: Adipocyte *Sirt1* deficiency causes insulin resistance on standard chow diet during aging. **A**: Body weight of WT and ATKO mice on standard chow diet during 60 weeks (NCD) (n = 10–15 per group). **B**: sqWAT, eWAT, BAT and liver weight of WT and ATKO mice on NCD. Values are expressed as means ± SEM (*P ≤ 0.05 **P ≤ 0.01 ***P < 0.001 vs. WT; n = 10/15). **C**: Mice body weight during the GTTs and ITTs. **D**: Glucose stimulated insulin secretion (GSIS). Plasma insulin concentration from WT and ATKO mice during IP-GTTs at the indicated time points. **E**: Intraperitoneal glucose tolerance tests (IP-GTT; 1 g/kg) and Area under curve (AUC) at 8 or 19 weeks of age (n = 8 per group). **F**: Intraperitoneal insulin tolerance tests (IP-ITTs; 0.6 U/kg) at 21 weeks of age (n = 8 per group). All of these studies were performed in the same cohort of mice. G: Glucose uptake of primary adipocytes from 15 weeks old mice, WT or ATKO, fed with NCD. Values are expressed as means ± SEM (*P ≤ 0.05, **P ≤ 0.01 *vs.* WT at the same time point).

3.3. The impact of adipocyte SIRT1 deletion on the metabolic response to HFD is time-dependent

Next, we studied the metabolic effects of adipocyte *Sirt1* deletion during short term and chronic HFD. WT and ATKO mice were fed 60% HFD for 5 weeks (short term; S) or 15 weeks (chronic; C) starting at 8 weeks of age. Body weight (BW) and adipose tissue mass were increased in ATKO mice compared to WT (Figure 3A,B), and this was evident in the first week of HFD and maintained throughout the treatment period. No differences in food intake were noted between the groups (Figure 3C). To further evaluate body composition changes, Dual energy X-ray absorptiometry (Dexa Scan) analyses were performed after 15 weeks of HFD (Figure 3D). ATKO mice exhibited increased total body area (TBA), fat mass, percentage of fat, and decreased bone mineral density (BMD), with no changes in lean body mass (LBM) compared to WT mice.

During the short term HFD feeding, ATKO mice showed exaggerated glucose intolerance, hyperinsulinemia and a reduced hypoglycemic effect of insulin compared to WT mice (Figure 4A–D). However, after chronic HFD feeding (15 weeks), ATKO mice were relatively more glucose tolerant and displayed an increased hypoglycemic response to insulin compared to WT (Figure 4A–D). In addition, basal insulin levels plateaued in the ATKO mice from short to chronic HFD, while they continued to increase in the WT mice with the development of obesity (Figure 4D), so that the ATKOs were no longer more hyperinsulinemic compared to WT. In other words, the metabolic dysfunction progressively worsened going from short term to chronic HFD in WT mice, whereas it plateaued, or improved, in the ATKO group. The result is that ATKO mice are less glucose tolerant and more insulin resistant than WT mice on short term HFD, but more glucose tolerant and less insulin resistant than WT mice on chronic HFD.

To further assess the difference in insulin sensitivity on chronic HFD, we performed hyperinsulinemic-euglycemic clamp studies in body weight matched WT and ATKO mice (Figure 4E). The glucose infusion rate (GIR) required to maintain euglycemia, and the ability of insulin to suppress hepatic glucose production (HGP) were both significantly increased in ATKO mice compared to WT mice. Insulin suppression of free fatty acid levels was slightly increased in ATKO mice (but not statistically significant). There was no impact on basal and insulin-stimulated glucose disposal rate (GDR and IS-GDR), suggesting muscle insulin sensitivity is not altered between groups. Consistent with the glucose clamp studies, insulin-stimulated Akt phosphorylation was significantly increased in liver and adipose tissue in ATKO mice compared with WT mice (Figure 4F,G). Thus, ATKO mice clearly display improved insulin sensitivity relative to WT mice after chronic HFD feeding, despite the increase in body weight and adiposity.

3.4. ATKO mice show reduced eWAT inflammation after chronic HFD

Inflammation is a key causative factor in insulin resistance [1]. Consistent with the relative insulin sensitive state of the chronic HFD ATKO mice, we found decreased inflammation both systemically (Figure 5A) and locally in epididymal adipose tissue (Figure 5B). ATKO mice had lower circulating levels of MCP-1, TNF-α and PAI-1 (Figure 5A) and lower expression of proinflammatory genes *Mcp-1*, *Tnf-α* (Figure 5B). Furthermore, increased expression of *Il-10*, an important anti-inflammatory gene and *Arginase*, a macrophage M2-associated marker, were detected in ATKO epididymal adipose tissue (Figure 5B,F).

We also measured the levels of FGF21 in plasma after chronic HFD feeding. FGF21 is a circulating factor, upregulated by fasting and HFD in liver and adipose tissue, that is associated with insulin sensitivity [25], plays a role in beigeing of adipose tissue [26] and also is selectively repressed by SIRT1 in adipocytes [27]. SIRT1 attenuates PPARγ activity in adipocytes resulting in decreased FGF21 production [27]. In our model, ATKO mice displayed higher

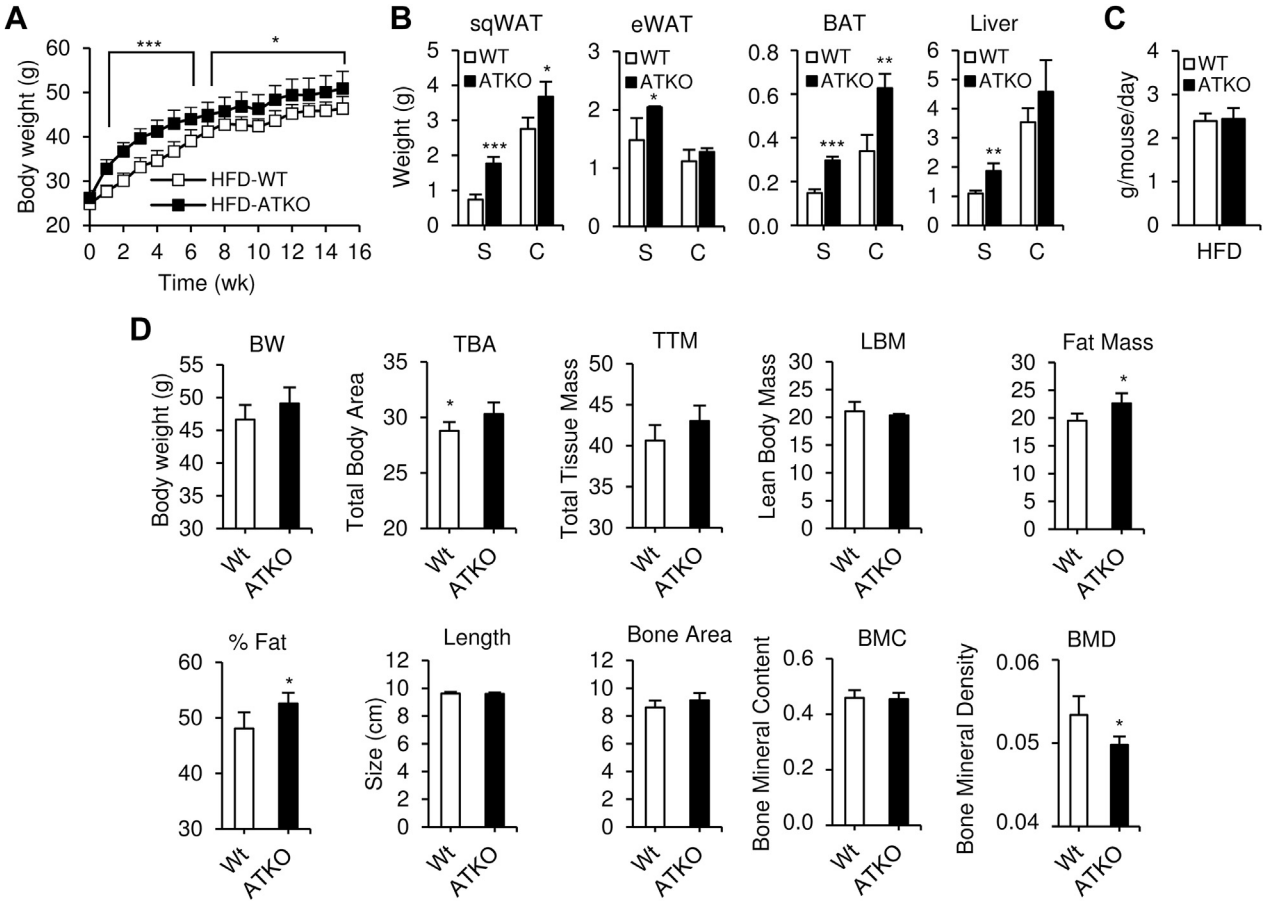

Figure 3: Body composition of *Sirt1* ATKO mice during HFD. **A**: Body weight of WT and *Sirt1* ATKO mice fed with 60% high fat diet (HFD) (n = 25–30 per group). **B**: sqWAT, eWAT, BAT and liver weight of WT and ATKO mice on short term or chronic HFD (S, Short term; C, Chronic). **C**: Food intake of *Sirt1* WT and ATKO mice at 5 weeks of HFD. **D**: Dual energy X-ray absorptiometry (DEXA). Body composition was assessed using DEXA scan (PIXImus2; Lunar, Madison, WI) and analyzed with PIXImus software (2.10; GE/Lunar) after 15 weeks of HFD. BW, body weight. TBA, Total body area. TTM, Total tissue mass. LBM, Lean body mass. Fat mass and percentage of fat. Length and bone area of the mice. BMC, Bone mineral content. BMD, Bone mineral density. Values are expressed as means ± SEM (*P < 0.05 *vs.* WT; n = 5/6 mice per group).

circulating levels of FGF21 (Figure 5A) as well as up-regulation of *Fgf21* gene expression in eWAT (Figure 5B). The elevated *Fgf21* expression, and particularly the increased circulating FGF21 levels, appear to provide at least one component for the insulin sensitivity in the chronic HFD ATKO mice. A similar upregulation was observed for *Ucp1*, a FGF21 target gene [28], in eWAT from ATKO mice fed HFD for an extended period of time (Figure 5C), as well as increased expression of other brown fat-selective genes, including *PGC1-α*, *Cox7a1* (Figure 5C).

To investigate the effect of ATKO on macrophage infiltration in eWAT, we performed immunostaining for the macrophage marker F4/80 and visualized the number of crown-like structures (CLS). Short term feeding of HFD to ATKO mice resulted in an increased number of CLSs (Figure 5D) and increased expression of macrophage markers CD68, CD11b, and CD11c (Figure 5F) compared with WT control mice. Interestingly, after chronic HFD feeding, ATKO mice exhibited reduced macrophage accumulation compared to WT, fully consistent with their relative insulin sensitivity at this time point (Figure 5E,F). Taken together, these results show that while inflammation continues to progress in WT mice between short term and chronic HFD feeding, this progression fails to occur in ATKO mice, resulting in a relative reduced inflammatory status compared with WT mice at the chronic time point.

3.5. ATKO mice show increased adipocyte hypertrophy/hyperplasia during HFD

In the early stages of HFD feeding, hypertrophy drives adipose tissue expansion in both eWAT and sqWAT. However, at more prolonged stages of HFD, only eWAT retains adipogenic capacity [29,30]. We studied the adipocyte-architecture in short term and chronically fed HFD ATKO and WT mice. The eWAT adipocytes from short term HFD-fed ATKO mice were significantly larger than from WT HFD fed mice (Figure 6A,B and C).During chronic HFD, the eWAT from ATKO mice underwent a significant change in adipocyte-architecture (Figure 6D). Adipocytes from ATKO mice were smaller (Figure 6B,E) with an overall ~25% decrease in average cell size compared to WT (Figure 6F). This suggests that hyperplasia plays a major role in eWAT expansion in ATKO mice, and that deletion of *Sirt1* partially protects from the hypertrophy seen in WT eWAT. These effects were specific to eWAT as no significant differences in cell size were observed in sqWAT or lipid droplet size in BAT (Figure 6G).

3.6. ATKO mice display PPARγ hyperactivity resulting from increased acetylation and reduced Ser273 phosphorylation

Enhanced adipogenic and anti-inflammatory responses in the adipose tissue can be induced by hyperactivity of PPARγ, a well characterized SIRT1 target. SIRT1 inhibits adipocyte differentiation by deacetylation

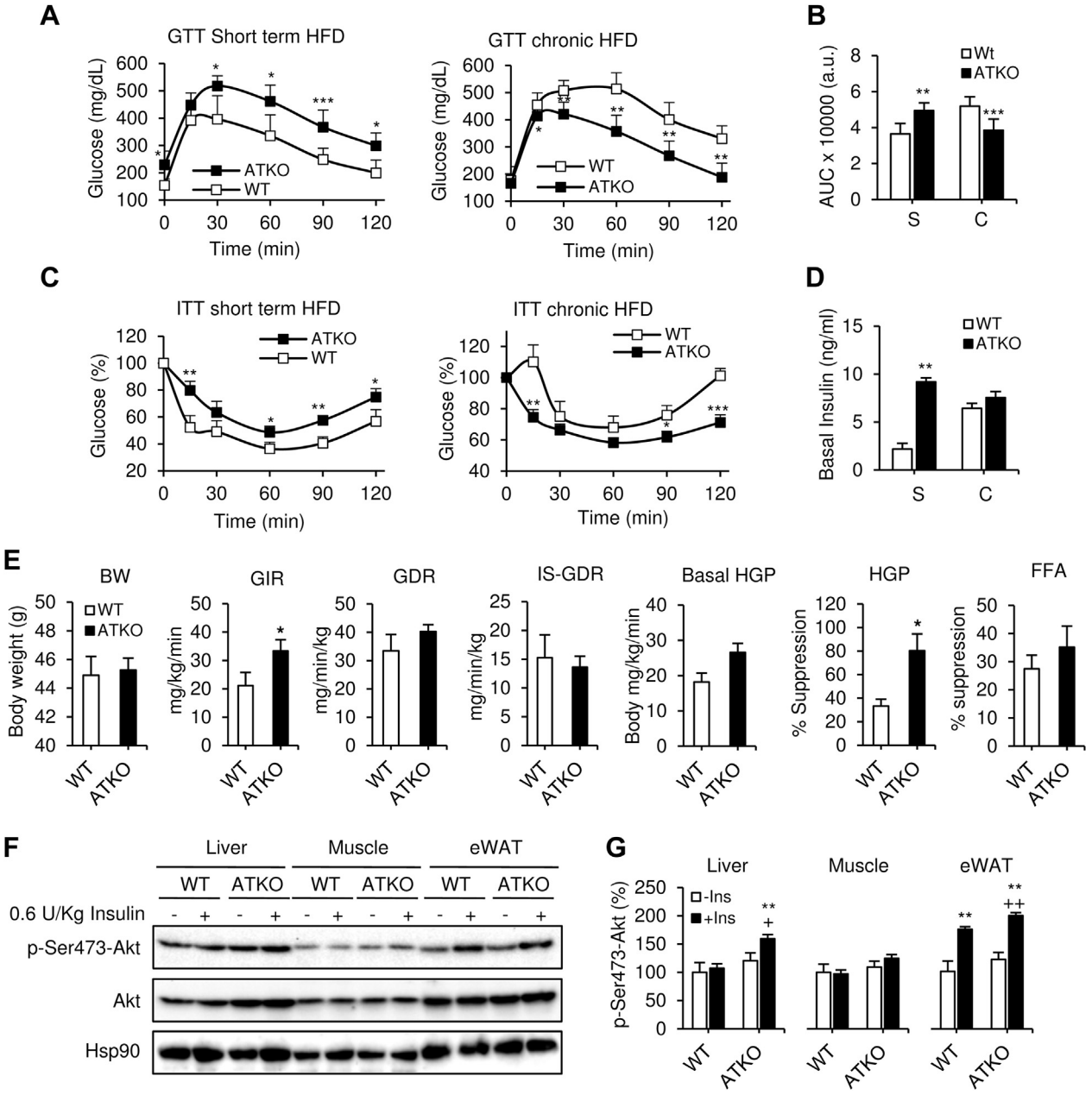

Figure 4: Dual effect of *Sirt1* deficiency in adipose tissue during HFD. Short term *vs.* chronic effects. **A, C**: Intraperitoneal glucose tolerance tests (IP-GTT; 1 g/kg) and intraperitoneal insulin tolerance tests (IP-ITT; 0.6 U/kg) during short term HFD feeding (S, 5 wks; n = 10–12 per group) and chronic HFD feeding (C, 15 wks; n = 10–12 per group). **B, D**: Area under curve (AUC) and basal insulin levels from previous GTTs. Values are expressed as means ± SEM (*P ≤ 0.05, **P ≤ 0.01 and ***P ≤ 0.001 *vs.* WT at the same time point). **E**: Hyperinsulinemic-euglycemic clamp study in chronic HFD-fed mice (15 weeks). BW, Body weight. WT and ATKO matched body weights of mice during clamp studies. GIR, glucose infusion rate during hyperinsulinemic-euglycemic clamp. GDR, Glucose disposal rate. IS-GDR, insulin-stimulated glucose disposal rate. Basal-HGP, basal hepatic glucose production rate. HGP-Suppression, percent suppression of HGP. FFA, Free fatty acid suppression. Values are expressed as means ± SEM (*P ≤ 0.05 *vs.* WT; n = 5/6 mice per group). **F**: Western blot showing acute insulin-stimulated phosphorylation of AKT in liver, muscle and eWAT from chronic HFD-fed mice. Hsp90 expression was used as loading control. The western blot shown is representative of four independent experiments. **G**: Densitometry analysis and ratio of phospho-Ser473-Akt/total Akt from **F**. Values are expressed as means ± SEM (*P ≤ 0.05 **P ≤ 0.001 *vs.* WT basal. $^{+}$P ≤ 0.05; $^{++}$P ≤ 0.001 *vs.* ATKO basal).

of PPARγ [8,31,32]. Consistent with this, ATKO mice showed enhanced PPARγ acetylation after both, short term and chronic HFD feeding (2.5 and 4.2 times higher respectively, Figure 7A). Interestingly, WT mice fed chronic HFD also displayed enhanced PPARγ acetylation (2.4x), most likely as a result of SIRT1 downregulation in adipose tissue [10]. Furthermore, we analyzed a subset of genes previously reported to be repressed by PPARγ [33], showed lower expression in ATKO mice during short term and chronic HFD, while in WT mice the downregulation is progressive (Figure 7B).

PPARγ activity is also regulated by phosphorylation of serine 273 by CDK5 [34]. CDK5 itself is activated by phosphorylation at tyrosine 15 and binding to the co-activator p25. In obesity and diabetes, pro-inflammatory signals lead to increased levels of cytoplasmic p25 with consequent activation of CDK5 and phosphorylation of PPARγ

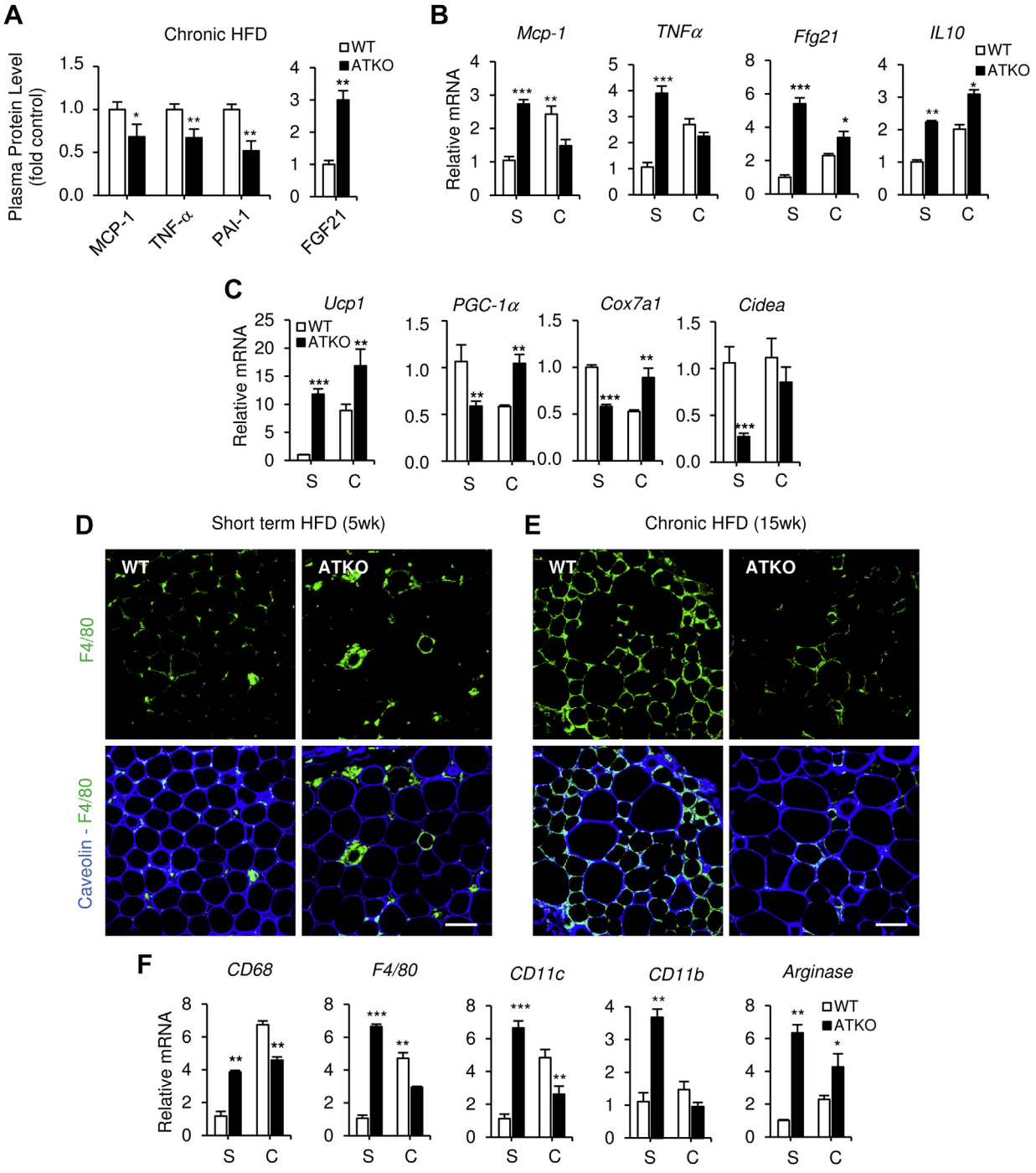

Figure 5: ATKO mice show reduced inflammation and infiltration in eWAT after prolonged HFD. **A**–**B**: Plasma protein and mRNA levels of inflammatory cytokines and chemokines measured by Milliplex during short term (S) or chronic HFD (C) (n = 8 per group). **C**: mRNA levels of brown fat-selective genes (Ucp1, PGC-1α, Cox7a1 and Cidea), anlayzed by qPCR. **D-E**: Immunofluorescence of eWAT from short term or chronic HFD-fed mice. Adipose tissue was stained with Caveolin as adipocyte membrane marker and F4/80 as macrophage cell marker. Scale bar is 100 μm (n = 4/5 per group). **F**: Gene expression of adipose tissue infiltration markers during HFD, analyzed by qPCR. Values are expressed as means ± SEM. (*P ≤ 0.05, **P ≤ 0.01, ***P ≤ 0.001 *vs.* WT at the same point, WT; n = 4/5 per group in qPCR and n = 10/12 per group for plasmatic cytokines).

[35]. Since PPARγ Ser273 phosphorylation is inhibitory, whereas dephosphorylation confers an active insulin sensitizer transcriptional program [16,18], we hypothesized that the enhanced insulin sensitivity observed in chronic HFD-fed *Sirt1* ATKO mice might be related to PPARγ phosphorylation status.

In normal chow and short term HFD fed mice, pSer273-PPARγ and pTyr15-CDK5 levels were increased consistent with the insulin resistant phenotype (Figure 7C,D). However, pSer273-PPARγ and pTyr15-CDK5 levels were reduced in ATKO compared to WT mice after 15 weeks of HFD feeding (Figure 7C,D). Furthermore, the set of genes

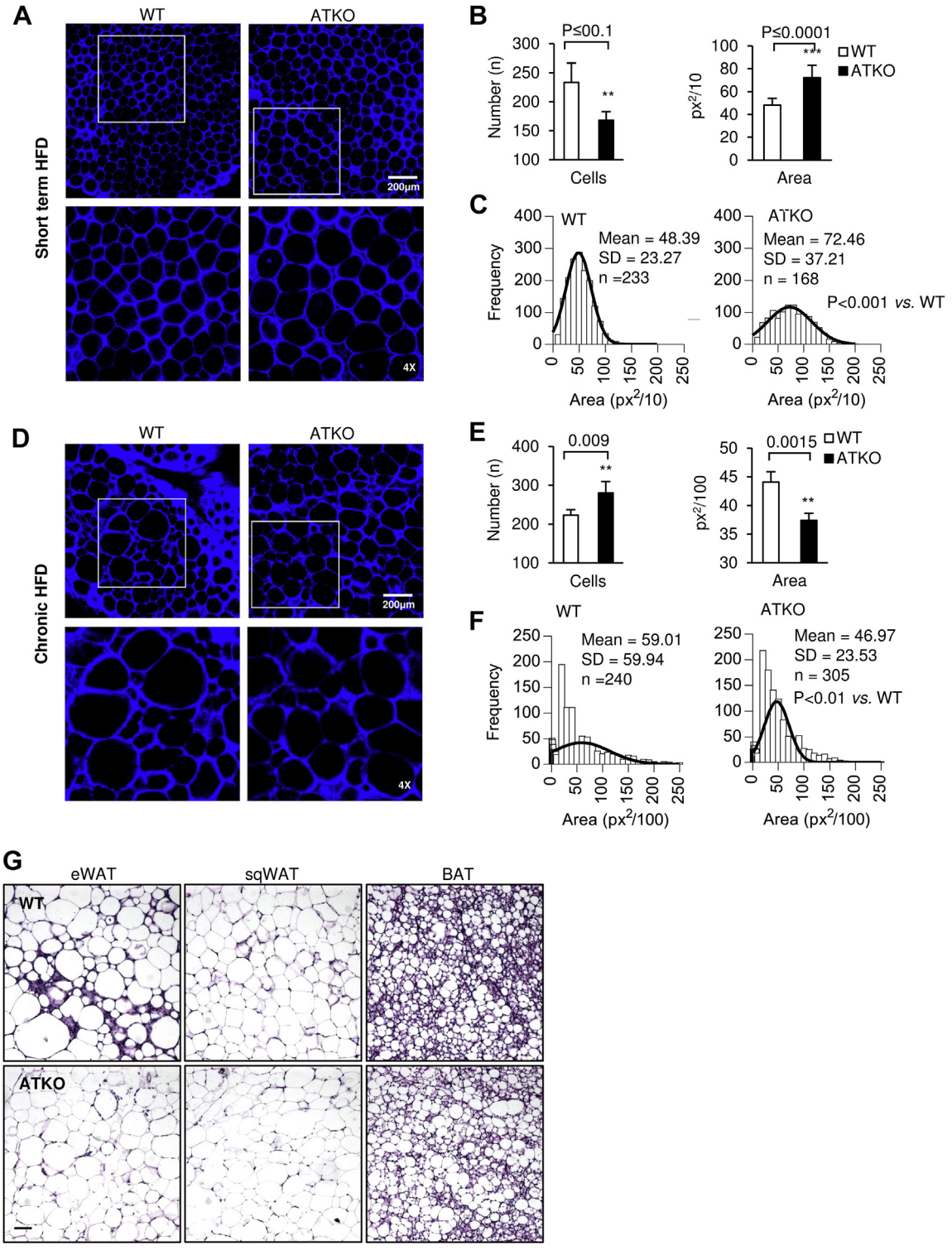

Figure 6: ATKO mice show higher hyperplasia during chronic HFD. **A**: Immunofluorescence of eWAT from short term HFD feeding. Adipose tissue was stained with Caveolin (blue) as adipocyte membrane marker. Scale bar is 200 µm. The images below are 4x magnification corresponding to the white box on the upper images. **B-C**: Quantification, area and adipocyte size frequency measurement from eWAT inmunofluorescence images. **D-F**: Same analysis in WT and ATKO eWAT from chronic HFD feeding mice. Values are expressed as means ± SEM. (n = 4 mice/group and 2 images/mouse were analyzed). **G**: Hematoxylin & Eosin of eWAT, sqWAT, and BAT from WT and ATKO mice from chronic HFD-fed mice. Fat tissues were fixed with 4% PFA, embedded in paraffin blocks and sectioned in the UCSD Mouse Phenotype Service Core (Moores Cancer Center, UCSD). Bright field photographs were taken using a Zeiss Observer.Z1 microscope. Scale bar is 100 µm. (n = 4 mice/group and 2 images/mouse were analyzed).

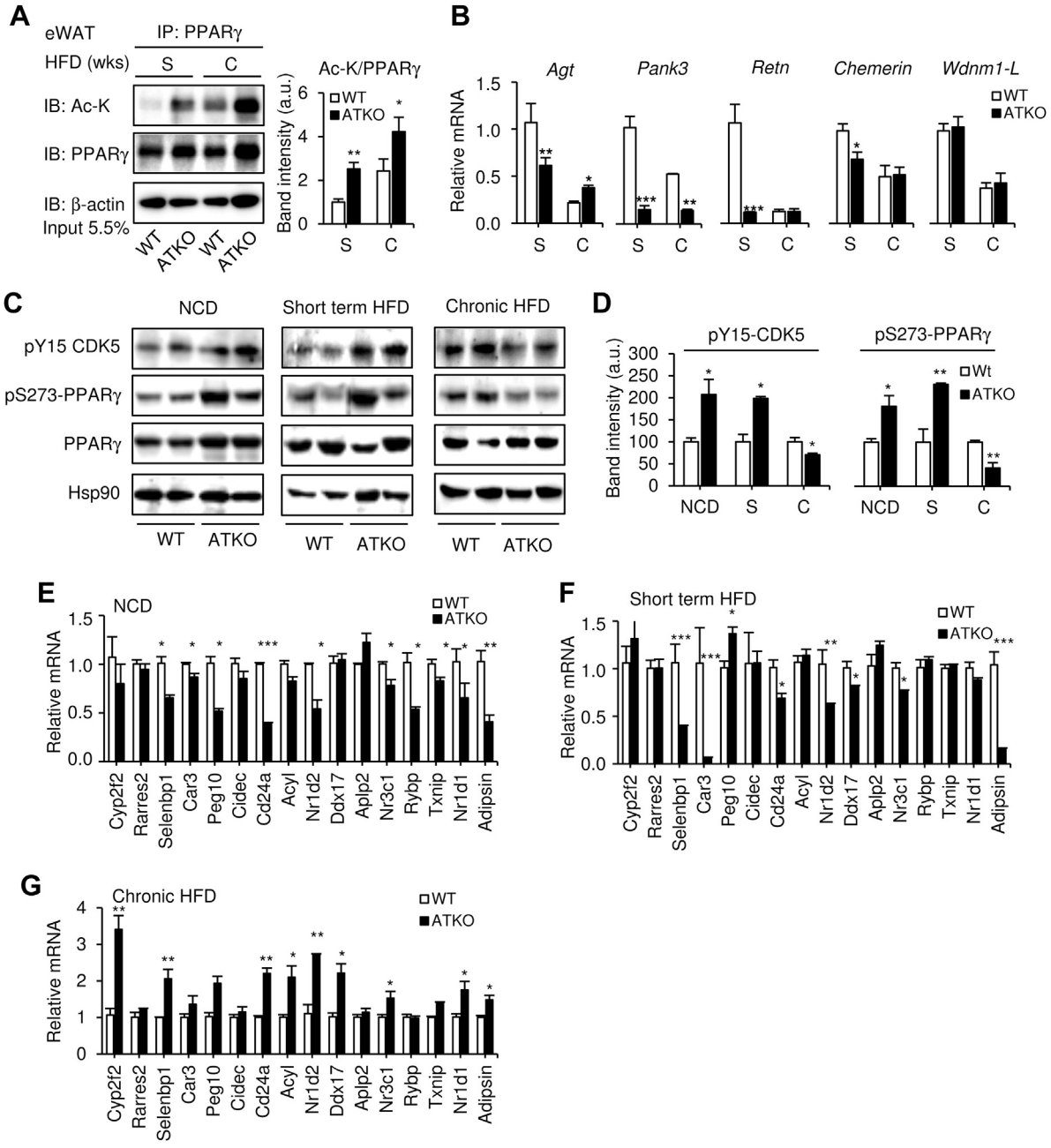

Figure 7: ATKO mice show reduced phosphorylation of PPARγ-Ser273 after chronic HFD feeding. **A**: Immunoprecipitation of PPARγ and western blot with antibodies to acetylated lysine (Ac-K) or PPARγ in eWAT from short term (S) or chronic (C) HFD-fed mice. β-actin was used as a loading control, and densitometry analysis is shown in the graph. One representative western blot selected from four independent experiments is shown. **B**: mRNA levels of genes know to be repressed by PPARγ (angiotensinogen [agt], Pank3, resistin [retn], chemerin and Wdnm1-like) analyzed by qPCR. **C**: CDK5 and PPARγ phosphorylation status in WT and ATKO mice fed with NCD or HFD measured by western blot at the indicated times. Hsp90 expression was used as loading control. **D**: Densitometry analysis and ratio of phospho-Y15-CDK5/Hsp90 and phospho-S273-PPARγ/PPARγ from Figure 7C (n = 4 per group). **E-G**: qPCR analysis of p-S273-PPARγ repressed genes in NCD-fed mice and short term or chronic HFD-fed mice (n = 4/5 per group). Values are expressed as means ± SEM. (*P ≤ 0.05, **P ≤ 0.01, ***P ≤ 0.001 *vs.* WT).

repressed by phosphorylated PPARγ described by Choi et al. were downregulated in ATKO mice fed NCD or short term HFD (Figure 7E,F) but were upregulated in ATKO following chronic HFD feeding (Figure 7G). Thus, we suggest that protection of ATKO mice from long-term impact of HFD feeding is due to PPARγ hyperacetylation and dephosphorylation, resulting in sustained PPARγ activity. This leads to reduced inflammation, decreased CDK5 phosphorylation and upregulation of genes involved in insulin sensitization (summarized in the Graphical Abstract).

4. DISCUSSION

It is well known that obesity leads to a state of chronic, sub-acute tissue inflammation with increased accumulation of adipose tissue

macrophages (ATMs) and this is a key driver of the insulin resistance syndrome [1,2,36]. Recently we have found that moderate and severe obesity were associated with a significant reduction in *Sirt1* mRNA expression and an increase in ATM content in human adipose tissue [10]. It has been reported that SIRT1 can exert anti-inflammatory effects and knockdown of *Sirt1 in vivo* using antisense-oligonucleotides (ASOs) promotes inflammation and ATM accumulation [10]. However, in these studies, macrophage-deficient mice showed a similar induction of inflammation after treatment with *Sirt1* ASO, suggesting that in addition to its influence on ATMs, SIRT1 activity might also be important in adipocytes. To address this question, we studied the role of adipocyte SIRT1 on inflammation, glucose metabolism and insulin resistance in adipocyte-specific *Sirt1* knock-out mice (ATKO) in the context of an acute or chronic HFD/obesity. Given the important anti-inflammatory effects of SIRT1 [9,24], we found, as expected, that NCD fed ATKO mice showed impaired glucose tolerance and were insulin resistant compared to WT controls. When challenged with a HFD, ATKO mice initially become more inflamed and developed glucose intolerance, hyperinsulinemia and insulin resistance faster than WT mice. Surprisingly, as the time period of HFD feeding continued, the ATKO mice phenotype plateaued while the WT mice continued to develop metabolic disease. Therefore, ATKO mice fed chronic HFD showed reduced inflammation, improved glucose tolerance and enhanced insulin sensitivity, relative to their control WT mice.

This phenotype was unexpected, and we were able to trace the mechanisms to increased PPARγ activity, higher adipogenesis and reduction of inflammation during the latter stages of HFD. Thus, in obesity, adipocyte PPARγ was largely hyperacetylated and unphosphorylated with a constitutively active state in the ATKO mice [34]. This was also associated with upregulation of brown fat-selective genes and induction of a variety of WAT target genes associated with insulin sensitization [18,33]. A decrease in the adiponectin secretion has been associated with insulin resistance in mouse models of impaired insulin sensitivity [37], and this effect was reproduced in our experiments in the WT HFD-fed mice. However, no significant changes were detected in ATKO HFD-fed mice between short or chronic HFD (data not shown), this may be due to the involvement of SirT1, FOXO1 and C/EBPα interaction in the adiponectin gene expression [38,39], and therefore, the reduction of adiponectin plasma levels in Wt HFD-fed mice could be related to the SIRT1 downregulation previously described in 3T3-L1 adipocytes and obesity/HFD [10,40].

Much attention has been given to the initiators of inflammation in obesity, with relatively little focus on the resolution of inflammation. Normally, tissue inflammation is resolved through a series of complex immune mechanisms [41]. In obesity, the chronic state of inflammation could be, at least in part, a reflection of inadequate resolution. Thus, in the normal obese state, resolution mechanisms come into play, but they might be inadequate to dissipate the inflammation and can only maintain a sub-acute chronic inflammatory state. Wernstedt Asterholm et al. have recently shown that adipose tissue inflammation is an adaptive response, essential for storage of excess nutrients and contributes to a healthy expansion and remodeling of the adipose tissue [42]. Also, Wang et al. have found that eWAT adipose tissue, but not sqWAT, undergoes hypertrophy first and hyperplasia later during chronic HFD [29]. In our model, during short term HFD, the ATKO mice displayed increased inflammation, coupled with eWAT hypertrophy compared to the WT (Figures 5 and 6). However, the population of adipocytes after chronic HFD is phenotypically different from those in the short term HFD and, therefore, by increasing adipogenesis, hyperplasia plays a major role in eWAT expansion in ATKO mice during chronic HFD (Figure 6). The exact mechanism underlying the proliferation of smaller, more insulin sensitive, adipocytes due to the *Sirt1* deletion in eWAT remains unclear, but we did find increased expression of Cd24 in ATKO mice during chronic HFD, which is a marker of adipocyte progenitor cells [43,44] (Figure 7H). This is also consistent with increased adipocyte PPARγ activity [45,46]. Indeed, it is known that PPARγ exhibits ligand-independent activation by protein acetylation through downregulation of SIRT1 [32], and the eWAT from ATKO mice showed high levels of acetylated PPARγ during chronic HFD. Although Boutant et al. recently found that SIRT1 improves glucose homeostasis by enhancing BAT function [47], we did not find significant differences in cell size or lipid droplet size in BAT (Figure 6G). Interestingly, Kusminski et al. found that during the initial stages of a HFD challenge, the outer mitochondrial membrane protein MitoNEET is necessary to induce the browning program to dissipate surplus dietary energy for up to 12 weeks [48]. However, after 12 weeks HFD, the adipocytes lose their ability to maintain the browning program and this is associated with adipocyte death [49]. This mechanism could relate to the increased expression of *Cd24* in ATKO mice.

In our model, during chronic HFD, ATKO mice exhibit a decrease in the inflammatory state with improvement in glucose tolerance. This raises the possibility that downregulation of SIRT1 plays a previously unknown role in long-term inflammation resolution mediated by PPARγ activation. An interesting mechanism that relates to the more insulin sensitive state in the ATKO mice after long-term HFD, could be related to the regulation of PPARγ activity by phosphorylation. It is known that PPARγ exhibits ligand-independent insulin sensitizing effects in the unphosphorylated state. Thus, Spiegelman et al. and others have demonstrated that PPARγ S273 phosphorylation is increased in the obese state and that CDK5, which is also activated in obesity and diabetes, can phosphorylate PPARγ at this site [18,35]. Unphosphorylated PPARγ induces a set of target genes which can promote insulin sensitivity. Indeed, treatment of cells or mice with classical and non-classical thiazolidinediones (TZDs) such as rosiglitazone or MRL24 respectively, prevents PPARγ phosphorylation, inducing a comparable target gene expression signature, along with systemic insulin sensitization [18]. Moreover, SIRT1 can be phosphorylated at serine 47 (S47) by CDK5, which inhibits its anti-inflammatory functions in endothelial cells and blocks the anti-senescence activity of SIRT1 [50]. This post-translational regulation of SIRT1 may contribute to the inflammatory phenotype in WT mice. In our studies, the reduction in inflammation of the chronic HFD ATKO mice might explain the decrease in CDK5 Tyr15 and PPARγ S273 phosphorylation. This process was associated with induction of the same set of PPARγ target genes reported by Spiegelman et al. [18]. Consistent with the studies of Accili et al., who showed that decreased PPARγ phosphorylation can be mediated by increased acetylation and therefore a reduction in inflammation, we also show that during chronic HFD adipocyte *Sirt1* deletion leads to hyperacetylation of PPARγ and low profile of phosphorylation, [51]. The regulation of PPARγ activity by phosphorylation in S273 (negatively) and acetylation in K268 and K293 (positively) are different mechanisms and they are not related directly. While the acetylation of PPARγ is p300/SIRT1 dependent, the phosphorylation in S273 is CDK5 dependent. Furthermore, CDK5 activity is regulated by its phosphorylation at Y15 and by calcium-dependent proteases (Calpains) that are highly activated in obesity, diabetes, atherosclerosis, and inflammation [35,52].

We have described that SIRT1 inhibits NFκB in macrophages and plays a role in adipose tissue inflammation [10]. NFκB induces expression of PTP1B, a negative regulator of insulin sensitivity [53], and SIRT1 represses PTP1B in insulin resistant obese mice improving insulin

sensitivity [54]. Since PTP1B deficiency increases glucose uptake [55,56], the decreased inflammation in chronic-HFD ATKO mice compared to WT mice could lead to decreased PTP1B expression with a resulting increase in insulin sensitivity. Moreover, SIRT1 deacetylates IRS2, enhancing its tyrosine phosphorylation [57,58]. The regulation of this two proteins by SIRT1 is important for insulin signaling in the liver and it would be of interest to study these events in the adipocyte.

Our short term HFD results are similar with those reported by Chalkiadaki et al. who also studied the effects of SIRT1 ablation in adipocytes [59]. However, in contrast to their findings, we observed an improvement in the metabolic phenotype relative to WT mice after chronic HFD feeding. While we cannot fully reconcile our results with these earlier studies, the models used are quite different. Chalkiadaki et al. studied female C57BL/6J mice [59], and these mice are known to be more resistant than males to HFD [60,61]. Furthermore, the mice were subjected to HFD immediately after weaning, whereas, we initiated the HFD at 8 weeks of age; it has been reported that early HFD advances the onset of puberty in females [62,63].

In these studies, we have used our aP2 Cre mice line to induce adipocyte-specific deletion of *Sirt1*. Three aP2 Cre mice lines exist [64], and some can exhibit variable degrees of target gene recombination in macrophages, which can be problematic for these kinds of metabolic studies [65,66]. However, the specific aP2 Cre line we used in these studies, and in our previous reports does not exhibit expression in muscle or liver [15,16,67–70], nor does it show macrophage expression, as also shown in the current paper (Figure 1C). In addition, many papers reporting data with this same aP2 Cre line agree with the high specificity ap2 Cre expression for adipocytes [59,71–74], and only one of has found gene recombination in endothelial cells of the heart and nonendothelial, nonmyocyte cells in skeletal muscle [75]. Therefore, the great predominance of data in this particular aP2 Cre line demonstrates no gene recombination in macrophages, muscle or liver, showing a high degree of adipocyte selectively. In the aP2 Cre model, it is important to note that aP2 expression occurs early in adipocyte progenitor cells, so that one cannot distinguish between developmental effects *vs.* effects on the mature adipocyte phenotype. Thus, it would be advantageous to compare these results to those obtained with adiponectin Cre mice since adiponectin is expressed only after adipocyte differentiation.

5. CONCLUSIONS

Our studies have shown that deletion of *Sirt1* from adipocytes leads to exaggerated insulin resistance, glucose intolerance and inflammation on short term HFD. These results are consistent with reports showing anti-inflammatory effects of SIRT1 and that pharmacologic activation of SIRT1 can lead to beneficial effects on glucose homeostasis. Thus, whole-body SIRT1 overexpression protects against genetically-induced obesity and from age-induced glucose intolerance [76]. In muscle cells, overexpression of SIRT1 increased insulin-induced Akt phosphorylation [77] and, in BAT, SIRT1 overexpression lead to increased energy expenditure [47]. Moreover, pharmacologic SIRT1 activation can reduce liver fat content and enhance systemic insulin sensitivity [3,78]. However, subsequent studies have shown that these SIRT1 activating compounds are not specific for this target and the efficacy in humans is controversial [79,80]. Consistent with our long-term HFD results, where ATKO mice became more insulin sensitive, glucose tolerant, and less inflamed than WT controls, ASO-mediated knockdown of *Sirt1* in the liver of diabetic rats decreases basal hepatic glucose and increases hepatic insulin sensitivity [81]. Reduction of *Sirt1* expression using shRNA in mouse liver also improves whole body insulin sensitivity [82]. Neuronal *Sirt1* deletion is protective against metabolic disease [23], and one recent report describes that inhibition of SIRT1 by RNAi or HDAC inhibitors promotes adipogenesis, and enhances insulin sensitivity [32]. We traced this phenotypic change to the acetylation/phosphorylation status of PPARγ (summarized in the Graphical Abstract). Future experiments comparing the gene expression pattern of the chronic HFD- SIRT1 ATKO mice with the pattern induced by TZD treatment, would be of interest in order to highlight commonalities and differences. These studies should inform potential SIRT1-based therapies, since such treatments would be chronic in nature and might have different effects over the long haul compared to the short term.

ACKNOWLEDGMENTS

We thank Jachelle M. Ofrecio and Sarah Nalbandian for their help with animal maintenance and Angela M. Tyler for editorial assistance. We thank the UCSD Histology Core lab for technical help with processing tissues specimens, and UCSD Microscope Resource for microscopy analysis. Ariane R. Pessentheiner was funding by Austrian Science Fund (FWF DK-MCD W1226) and Marshall plan Scholarship. Paqui G. Traves was funding by the Marie Curie International Outgoing Fellowship Program (FP7-PEOPLE-2011-IOF).

This study was funded in part by the National Institutes of Health, United States grants NIDDK DK033651 (J.M.O.), DK063491 (J.M.O.), DK074868 (J.M.O.), and the Eunice Kennedy Shriver NICHD/NIH through a cooperative agreement U54 HD 012303-25 as part of the specialized Cooperative Centers Program in Reproduction and Infertility Research.

R.M. researched data, wrote the manuscript, and reviewed and edited the manuscript. O.O., A.M.J., P.G.T., and A.P. researched data and reviewed and edited the manuscript. J.M.N., D.Y.O., C.LL.I., H.C., P.L., G.B., and J.R.C. researched data. L.Q. and D.A. reviewed and contributed to discussion. J.M.O. wrote the manuscript, contributed to discussion and reviewed and edited the manuscript. Authors declare no conflict of interest. J.M.O. is the guarantor of this work and, as such, had full access to all the data in the study and takes responsibility for the integrity of the data and the accuracy of the data analysis.

CONFLICT OF INTEREST

None declared.

APPENDIX A. SUPPLEMENTARY DATA

Supplementary data related to this article can be found at http://dx.doi.org/10.1016/j.molmet.2015.02.007

REFERENCES

[1] Johnson, A.M., Olefsky, J.M., 2013. The origins and drivers of insulin resistance. Cell 152(4):673–684. http://dx.doi.org/10.1016/j.cell.2013.01.041.

[2] Olefsky, J.M., Glass, C.K., 2010. Macrophages, inflammation, and insulin resistance. Annual Review of Physiology 72:219–246. http://dx.doi.org/10.1146/annurev-physiol-021909-135846.

[3] Haigis, M.C., Sinclair, D.A., 2010. Mammalian sirtuins: biological insights and disease relevance. Annual Review of Pathology 5:253–295. http://dx.doi.org/10.1146/annurev.pathol.4.110807.092250.

[4] McBurney, M.W., Clark-Knowles, K.V., Caron, A.Z., Gray, D.A., 2013. SIRT1 is a highly networked protein that mediates the adaptation to chronic physiological stress. Genes & Cancer 4(3–4):125–134. http://dx.doi.org/10.1177/1947601912474893.

[5] Rodgers, J.T., Lerin, C., Haas, W., Gygi, S.P., Spiegelman, B.M., Puigserver, P., 2005. Nutrient control of glucose homeostasis through a complex of PGC-

1alpha and SIRT1. Nature 434(7029):113–118. http://dx.doi.org/10.1038/nature03354.

[6] Kanfi, Y., Peshti, V., Gozlan, Y.M., Rathaus, M., Gil, R., Cohen, H.Y., 2008. Regulation of SIRT1 protein levels by nutrient availability. FEBS Letters 582(16):2417–2423. http://dx.doi.org/10.1016/j.febslet.2008.06.005.

[7] Silva, J.P., Wahlestedt, C., 2010. Role of Sirtuin 1 in metabolic regulation. Drug Discovery Today 15(17–18):781–791. http://dx.doi.org/10.1016/j.drudis.2010.07.001.

[8] Picard, F., Kurtev, M., Chung, N., Topark-Ngarm, A., Senawong, T., Machado De Oliveira, R., et al., 2004. Sirt1 promotes fat mobilization in white adipocytes by repressing PPAR-gamma. Nature 429(6993):771–776. http://dx.doi.org/10.1038/nature02583.

[9] Yoshizaki, T., Milne, J.C., Imamura, T., Schenk, S., Sonoda, N., Babendure, J.L., et al., 2009. SIRT1 exerts anti-inflammatory effects and improves insulin sensitivity in adipocytes. Molecular and Cellular Biology 29(5):1363–1374. http://dx.doi.org/10.1128/MCB.00705-08.

[10] Gillum, M.P., Kotas, M.E., Erion, D.M., Kursawe, R., Chatterjee, P., Nead, K.T., et al., 2011. SirT1 regulates adipose tissue inflammation. Diabetes 60(12):3235–3245. http://dx.doi.org/10.2337/db11-0616.

[11] Park, S.J., Ahmad, F., Philp, A., Baar, K., Williams, T., Luo, H., et al., 2012. Resveratrol ameliorates aging-related metabolic phenotypes by inhibiting cAMP phosphodiesterases. Cell 148(3):421–433. http://dx.doi.org/10.1016/j.cell.2012.01.017.

[12] Poulsen, M.M., Vestergaard, P.F., Clasen, B.F., Radko, Y., Christensen, L.P., Stodkilde-Jorgensen, H., et al., 2013. High-dose resveratrol supplementation in obese men: an investigator-initiated, randomized, placebo-controlled clinical trial of substrate metabolism, insulin sensitivity, and body composition. Diabetes 62(4):1186–1195. http://dx.doi.org/10.2337/db12-0975.

[13] Spiegelman, B.M., 1998. PPAR-gamma: adipogenic regulator and thiazolidinedione receptor. Diabetes 47(4):507–514.

[14] Cheng, H.L., Mostoslavsky, R., Saito, S., Manis, J.P., Gu, Y., Patel, P., et al., 2003. Developmental defects and p53 hyperacetylation in Sir2 homolog (SIRT1)-deficient mice. Proceedings of the National Academy of Sciences of the United States of America 100(19):10794–10799. http://dx.doi.org/10.1073/pnas.1934713100.

[15] He, W., Barak, Y., Hevener, A., Olson, P., Liao, D., Le, J., et al., 2003. Adipose-specific peroxisome proliferator-activated receptor gamma knockout causes insulin resistance in fat and liver but not in muscle. Proceedings of the National Academy of Sciences of the United States of America 100(26):15712–15717. http://dx.doi.org/10.1073/pnas.2536828100.

[16] Li, P., Fan, W., Xu, J., Lu, M., Yamamoto, H., Auwerx, J., et al., 2011. Adipocyte NCoR knockout decreases PPARgamma phosphorylation and enhances PPAR gamma activity and insulin sensitivity. Cell 147(4):815–826. http://dx.doi.org/10.1016/j.cell.2011.09.050.

[17] Rodriguez-Prados, J.C., Traves, P.G., Cuenca, J., Rico, D., Aragones, J., Martin-Sanz, P., et al., 2010. Substrate fate in activated macrophages: a comparison between innate, classic, and alternative activation. Journal of Immunology 185(1):605–614. http://dx.doi.org/10.4049/jimmunol.0901698.

[18] Choi, J.H., Banks, A.S., Estall, J.L., Kajimura, S., Bostrom, P., Laznik, D., et al., 2010. Anti-diabetic drugs inhibit obesity-linked phosphorylation of PPAR-gamma by Cdk5. Nature 466(7305):451–456. http://dx.doi.org/10.1038/nature09291.

[19] Mayoral, R., Valverde, A.M., Llorente Izquierdo, C., Gonzalez-Rodriguez, A., Bosca, L., Martin-Sanz, P., 2010. Impairment of transforming growth factor beta signaling in caveolin-1-deficient hepatocytes: role in liver regeneration. The Journal of Biological Chemistry 285(6):3633–3642. http://dx.doi.org/10.1074/jbc.M109.072900.

[20] Osborn, O., Oh, D.Y., McNelis, J., Sanchez-Alavez, M., Talukdar, S., Lu, M., et al., 2012. G protein-coupled receptor 21 deletion improves insulin sensitivity in diet-induced obese mice. The Journal of Clinical Investigation 122(7):2444–2453. http://dx.doi.org/10.1172/JCI61953.

[21] Talukdar, S., Oh da, Y., Bandyopadhyay, G., Li, D., Xu, J., McNelis, J., et al., 2012. Neutrophils mediate insulin resistance in mice fed a high-fat diet through secreted elastase. Nature Medicine 18(9):1407–1412. http://dx.doi.org/10.1038/nm.2885.

[22] Oh, D.Y., Talukdar, S., Bae, E.J., Imamura, T., Morinaga, H., Fan, W., et al., 2010. GPR120 is an omega-3 fatty acid receptor mediating potent anti-inflammatory and insulin-sensitizing effects. Cell 142(5):687–698. http://dx.doi.org/10.1016/j.cell.2010.07.041.

[23] Lu, M., Sarruf, D.A., Li, P., Osborn, O., Sanchez-Alavez, M., Talukdar, S., et al., 2013. Neuronal Sirt1 deficiency increases insulin sensitivity in both brain and peripheral tissues. The Journal of Biological Chemistry 288(15):10722–10735. http://dx.doi.org/10.1074/jbc.M112.443606.

[24] Yoshizaki, T., Schenk, S., Imamura, T., Babendure, J.L., Sonoda, N., Bae, E.J., et al., 2010. SIRT1 inhibits inflammatory pathways in macrophages and modulates insulin sensitivity. American Journal of Physiology Endocrinology and Metabolism 298(3):E419–E428. http://dx.doi.org/10.1152/ajpendo.00417.2009.

[25] Muise, E.S., Azzolina, B., Kuo, D.W., El-Sherbeini, M., Tan, Y., Yuan, X., et al., 2008. Adipose fibroblast growth factor 21 is up-regulated by peroxisome proliferator-activated receptor gamma and altered metabolic states. Molecular Pharmacology 74(2):403–412. http://dx.doi.org/10.1124/mol.108.044826.

[26] Fisher, F.M., Kleiner, S., Douris, N., Fox, E.C., Mepani, R.J., Verdeguer, F., et al., 2012. FGF21 regulates PGC-1alpha and browning of white adipose tissues in adaptive thermogenesis. Genes & Development 26(3):271–281. http://dx.doi.org/10.1101/gad.177857.111.

[27] Wang, H., Qiang, L., Farmer, S.R., 2008. Identification of a domain within peroxisome proliferator-activated receptor gamma regulating expression of a group of genes containing fibroblast growth factor 21 that are selectively repressed by SIRT1 in adipocytes. Molecular and Cellular Biology 28(1):188–200. http://dx.doi.org/10.1128/MCB.00992-07.

[28] Emanuelli, B., Vienberg, S.G., Smyth, G., Cheng, C., Stanford, K.I., Arumugam, M., et al., 2014. Interplay between FGF21 and insulin action in the liver regulates metabolism. The Journal of Clinical Investigation 124(2):515–527. http://dx.doi.org/10.1172/JCI67353.

[29] Wang, Q.A., Tao, C., Gupta, R.K., Scherer, P.E., 2013. Tracking adipogenesis during white adipose tissue development, expansion and regeneration. Nature Medicine 19(10):1338–1344. http://dx.doi.org/10.1038/nm.3324.

[30] Jernas, M., Palming, J., Sjoholm, K., Jennische, E., Svensson, P.A., Gabrielsson, B.G., et al., 2006. Separation of human adipocytes by size: hypertrophic fat cells display distinct gene expression. FASEB Journal: Official Publication of the Federation of American Societies for Experimental Biology 20(9):1540–1542. http://dx.doi.org/10.1096/fj.05-5678fje.

[31] Schug, T.T., Li, X., 2011. Sirtuin 1 in lipid metabolism and obesity. Annals of Medicine 43(3):198–211. http://dx.doi.org/10.3109/07853890.2010.547211.

[32] Jiang, X., Ye, X., Guo, W., Lu, H., Gao, Z., 2014. Inhibition of HDAC3 promotes ligand-independent PPARgamma activation by protein acetylation. Journal of Molecular Endocrinology 53(2):191–200. http://dx.doi.org/10.1530/JME-14-0066.

[33] Vernochet, C., Peres, S.B., Davis, K.E., McDonald, M.E., Qiang, L., Wang, H., et al., 2009. C/EBPalpha and the corepressors CtBP1 and CtBP2 regulate repression of select visceral white adipose genes during induction of the brown phenotype in white adipocytes by peroxisome proliferator-activated receptor gamma agonists. Molecular and Cellular Biology 29(17):4714–4728. http://dx.doi.org/10.1128/MCB.01899-08.

[34] Ahmadian, M., Suh, J.M., Hah, N., Liddle, C., Atkins, A.R., Downes, M., et al., 2013. PPARgamma signaling and metabolism: the good, the bad and the future. Nature Medicine 19(5):557–566. http://dx.doi.org/10.1038/nm.3159.

[35] Nohara, A., Okada, S., Ohshima, K., Pessin, J.E., Mori, M., 2011. Cyclin-dependent kinase-5 is a key molecule in tumor necrosis factor-alpha-induced insulin resistance. The Journal of Biological Chemistry 286(38):33457–33465. http://dx.doi.org/10.1074/jbc.M111.231431.

[36] Donath, M.Y., Shoelson, S.E., 2011. Type 2 diabetes as an inflammatory disease. Nature Reviews Immunology 11(2):98—107. http://dx.doi.org/10.1038/nri2925.

[37] Yamauchi, T., Kamon, J., Waki, H., Terauchi, Y., Kubota, N., Hara, K., et al., 2001. The fat-derived hormone adiponectin reverses insulin resistance associated with both lipoatrophy and obesity. Nature Medicine 7(8):941—946. http://dx.doi.org/10.1038/90984.

[38] Qiao, L., Shao, J., 2006. SIRT1 regulates adiponectin gene expression through Foxo1-C/enhancer-binding protein alpha transcriptional complex. The Journal of Biological Chemistry 281(52):39915—39924. http://dx.doi.org/10.1074/jbc.M607215200.

[39] Banks, A.S., Kon, N., Knight, C., Matsumoto, M., Gutierrez-Juarez, R., Rossetti, L., et al., 2008. SirT1 gain of function increases energy efficiency and prevents diabetes in mice. Cell Metabolism 8(4):333—341. http://dx.doi.org/10.1016/j.cmet.2008.08.014.

[40] Qiang, L., Wang, H., Farmer, S.R., 2007. Adiponectin secretion is regulated by SIRT1 and the endoplasmic reticulum oxidoreductase Ero1-L alpha. Molecular and Cellular Biology 27(13):4698—4707. http://dx.doi.org/10.1128/MCB.02279-06.

[41] Gonzalez-Periz, A., Claria, J., 2010. Resolution of adipose tissue inflammation. The ScientificWorld Journal 10:832—856. http://dx.doi.org/10.1100/tsw.2010.77.

[42] Wernstedt Asterholm, I., Tao, C., Morley, T.S., Wang, Q.A., Delgado-Lopez, F., Wang, Z.V., et al., 2014. Adipocyte inflammation is essential for healthy adipose tissue expansion and remodeling. Cell Metabolism 20(1):103—118. http://dx.doi.org/10.1016/j.cmet.2014.05.005.

[43] Park, K.W., Halperin, D.S., Tontonoz, P., 2008. Before they were fat: adipocyte progenitors. Cell Metabolism 8(6):454—457. http://dx.doi.org/10.1016/j.cmet.2008.11.001.

[44] Berry, R., Rodeheffer, M.S., 2013. Characterization of the adipocyte cellular lineage in vivo. Nature Cell Biology 15(3):302—308. http://dx.doi.org/10.1038/ncb2696.

[45] Stienstra, R., Duval, C., Muller, M., Kersten, S., 2007. PPARs, obesity, and inflammation. PPAR Research 2007:95974. http://dx.doi.org/10.1155/2007/95974.

[46] Delerive, P., Fruchart, J.C., Staels, B., 2001. Peroxisome proliferator-activated receptors in inflammation control. The Journal of Endocrinology 169(3):453—459.

[47] Boutant, M., Joffraud, M., Kulkarni, S.S., Garcia-Casarrubios, E., Garcia-Roves, P.M., Ratajczak, J., et al., 2015. SIRT1 enhances glucose tolerance by potentiating brown adipose tissue function. Molecular Metabolism 4(2):118—131. http://dx.doi.org/10.1016/j.molmet.2014.12.008.

[48] Kusminski, C.M., Park, J., Scherer, P.E., 2014. MitoNEET-mediated effects on browning of white adipose tissue. Nature Communications 5:3962. http://dx.doi.org/10.1038/ncomms4962.

[49] Strissel, K.J., Stancheva, Z., Miyoshi, H., Perfield 2nd, J.W., DeFuria, J., Jick, Z., et al., 2007. Adipocyte death, adipose tissue remodeling, and obesity complications. Diabetes 56(12):2910—2918. http://dx.doi.org/10.2337/db07-0767.

[50] Bai, B., Vanhoutte, P.M., Wang, Y., 2014. Loss-of-SIRT1 function during vascular ageing: hyperphosphorylation mediated by cyclin-dependent kinase 5. Trends in Cardiovascular Medicine 24(2):81—84. http://dx.doi.org/10.1016/j.tcm.2013.07.001.

[51] Qiang, L., Wang, L., Kon, N., Zhao, W., Lee, S., Zhang, Y., et al., 2012. Brown remodeling of white adipose tissue by SirT1-dependent deacetylation of Ppargamma. Cell 150(3):620—632. http://dx.doi.org/10.1016/j.cell.2012.06.027.

[52] Ahmed, D., Sharma, M., 2011. Cyclin-dependent kinase 5/p35/p39: a novel and imminent therapeutic target for diabetes mellitus. International Journal of Endocrinology 2011:530274. http://dx.doi.org/10.1155/2011/530274.

[53] Zabolotny, J.M., Kim, Y.B., Welsh, L.A., Kershaw, E.E., Neel, B.G., Kahn, B.B., 2008. Protein-tyrosine phosphatase 1B expression is induced by inflammation in vivo. The Journal of Biological Chemistry 283(21):14230—14241. http://dx.doi.org/10.1074/jbc.M800061200.

[54] Sun, C., Zhang, F., Ge, X., Yan, T., Chen, X., Shi, X., et al., 2007. SIRT1 improves insulin sensitivity under insulin-resistant conditions by repressing PTP1B. Cell Metabolism 6(4):307—319. http://dx.doi.org/10.1016/j.cmet.2007.08.014.

[55] Mobasher, M.A., de Toro-Martin, J., Gonzalez-Rodriguez, A., Ramos, S., Letzig, L.G., James, L.P., et al., 2014. Essential role of protein-tyrosine phosphatase 1B in the modulation of insulin signaling by acetaminophen in hepatocytes. The Journal of Biological Chemistry 289(42):29406—29419. http://dx.doi.org/10.1074/jbc.M113.539189.

[56] Gonzalez-Rodriguez, A., Nevado, C., Escriva, F., Sesti, G., Rondinone, C.M., Benito, M., et al., 2008. PTP1B deficiency increases glucose uptake in neonatal hepatocytes: involvement of IRA/GLUT2 complexes. American Journal of Physiology Gastrointestinal and Liver Physiology 295(2):G338—G347. http://dx.doi.org/10.1152/ajpgi.00514.2007.

[57] Zhang, J., 2007. The direct involvement of SirT1 in insulin-induced insulin receptor substrate-2 tyrosine phosphorylation. The Journal of Biological Chemistry 282(47):34356—34364. http://dx.doi.org/10.1074/jbc.M706644200.

[58] Valverde, A.M., Gonzalez-Rodriguez, A., 2011. IRS2 and PTP1B: two opposite modulators of hepatic insulin signalling. Archives of Physiology and Biochemistry 117(3):105—115. http://dx.doi.org/10.3109/13813455.2011.557386.

[59] Chalkiadaki, A., Guarente, L., 2012. High-fat diet triggers inflammation-induced cleavage of SIRT1 in adipose tissue to promote metabolic dysfunction. Cell Metabolism 16(2):180—188. http://dx.doi.org/10.1016/j.cmet.2012.07.003.

[60] Pettersson, U.S., Walden, T.B., Carlsson, P.O., Jansson, L., Phillipson, M., 2012. Female mice are protected against high-fat diet induced metabolic syndrome and increase the regulatory T cell population in adipose tissue. PloS One 7(9):e46057. http://dx.doi.org/10.1371/journal.pone.0046057.

[61] Hwang, L.L., Wang, C.H., Li, T.L., Chang, S.D., Lin, L.C., Chen, C.P., et al., 2010. Sex differences in high-fat diet-induced obesity, metabolic alterations and learning, and synaptic plasticity deficits in mice. Obesity 18(3):463—469. http://dx.doi.org/10.1038/oby.2009.273.

[62] Sanchez-Garrido, M.A., Castellano, J.M., Ruiz-Pino, F., Garcia-Galiano, D., Manfredi-Lozano, M., Leon, S., et al., 2013. Metabolic programming of puberty: sexually dimorphic responses to early nutritional challenges. Endocrinology 154(9):3387—3400. http://dx.doi.org/10.1210/en.2012-2157.

[63] Gout, J., Sarafian, D., Mutel, E., Vigier, M., Rajas, F., Mithieux, G., et al., 2010. Metabolic and melanocortin gene expression alterations in male offspring of obese mice. Molecular and Cellular Endocrinology 319(1—2):99—108. http://dx.doi.org/10.1016/j.mce.2010.01.021.

[64] Kang, S., Kong, X., Rosen, E.D., 2014. Adipocyte-specific transgenic and knockout models. Methods in Enzymology 537:1—16. http://dx.doi.org/10.1016/B978-0-12-411619-1.00001-X.

[65] Garcia-Arcos, I., Hiyama, Y., Drosatos, K., Bharadwaj, K.G., Hu, Y., Son, N.H., et al., 2013. Adipose-specific lipoprotein lipase deficiency more profoundly affects brown than white fat biology. The Journal of Biological Chemistry 288(20):14046—14058. http://dx.doi.org/10.1074/jbc.M113.469270.

[66] Paschos, G.K., Ibrahim, S., Song, W.L., Kunieda, T., Grant, G., Reyes, T.M., et al., 2012. Obesity in mice with adipocyte-specific deletion of clock component Arntl. Nature Medicine 18(12):1768—1777. http://dx.doi.org/10.1038/nm.2979.

[67] Barak, Y., Liao, D., He, W., Ong, E.S., Nelson, M.C., Olefsky, J.M., et al., 2002. Effects of peroxisome proliferator-activated receptor delta on placentation, adiposity, and colorectal cancer. Proceedings of the National Academy of Sciences of the United States of America 99(1):303—308. http://dx.doi.org/10.1073/pnas.012610299.

[68] Qi, L., Saberi, M., Zmuda, E., Wang, Y., Altarejos, J., Zhang, X., et al., 2009. Adipocyte CREB promotes insulin resistance in obesity. Cell Metabolism 9(3): 277–286. http://dx.doi.org/10.1016/j.cmet.2009.01.006.

[69] Sugii, S., Olson, P., Sears, D.D., Saberi, M., Atkins, A.R., Barish, G.D., et al., 2009. PPARgamma activation in adipocytes is sufficient for systemic insulin sensitization. Proceedings of the National Academy of Sciences of the United States of America 106(52):22504–22509. http://dx.doi.org/10.1073/pnas.0912487106.

[70] Lee, Y.S., Kim, J.W., Osborne, O., Oh da, Y., Sasik, R., Schenk, S., et al., 2014. Increased adipocyte O2 consumption triggers HIF-1alpha, causing inflammation and insulin resistance in obesity. Cell 157(6):1339–1352. http://dx.doi.org/10.1016/j.cell.2014.05.012.

[71] Sabio, G., Das, M., Mora, A., Zhang, Z., Jun, J.Y., Ko, H.J., et al., 2008. A stress signaling pathway in adipose tissue regulates hepatic insulin resistance. Science 322(5907):1539–1543. http://dx.doi.org/10.1126/science.1160794.

[72] Polak, P., Cybulski, N., Feige, J.N., Auwerx, J., Ruegg, M.A., Hall, M.N., 2008. Adipose-specific knockout of raptor results in lean mice with enhanced mitochondrial respiration. Cell Metabolism 8(5):399–410. http://dx.doi.org/10.1016/j.cmet.2008.09.003.

[73] Ahmadian, M., Abbott, M.J., Tang, T., Hudak, C.S., Kim, Y., Bruss, M., et al., 2011. Desnutrin/ATGL is regulated by AMPK and is required for a brown adipose phenotype. Cell Metabolism 13(6):739–748. http://dx.doi.org/10.1016/j.cmet.2011.05.002.

[74] Rohm, M., Sommerfeld, A., Strzoda, D., Jones, A., Sijmonsma, T.P., Rudofsky, G., et al., 2013. Transcriptional cofactor TBLR1 controls lipid mobilization in white adipose tissue. Cell Metabolism 17(4):575–585. http://dx.doi.org/10.1016/j.cmet.2013.02.010.

[75] Lee, K.Y., Russell, S.J., Ussar, S., Boucher, J., Vernochet, C., Mori, M.A., et al., 2013. Lessons on conditional gene targeting in mouse adipose tissue. Diabetes 62(3):864–874. http://dx.doi.org/10.2337/db12-1089.

[76] Herranz, D., Munoz-Martin, M., Canamero, M., Mulero, F., Martinez-Pastor, B., Fernandez-Capetillo, O., et al., 2010. Sirt1 improves healthy ageing and protects from metabolic syndrome-associated cancer. Nature Communications 1:3. http://dx.doi.org/10.1038/ncomms1001.

[77] Frojdo, S., Durand, C., Molin, L., Carey, A.L., El-Osta, A., Kingwell, B.A., et al., 2011. Phosphoinositide 3-kinase as a novel functional target for the regulation of the insulin signaling pathway by SIRT1. Molecular and Cellular Endocrinology 335(2):166–176. http://dx.doi.org/10.1016/j.mce.2011.01.008.

[78] Purushotham, A., Schug, T.T., Xu, Q., Surapureddi, S., Guo, X., Li, X., 2009. Hepatocyte-specific deletion of SIRT1 alters fatty acid metabolism and results in hepatic steatosis and inflammation. Cell Metabolism 9(4):327–338. http://dx.doi.org/10.1016/j.cmet.2009.02.006.

[79] Hubbard, B.P., Gomes, A.P., Dai, H., Li, J., Case, A.W., Considine, T., et al., 2013. Evidence for a common mechanism of SIRT1 regulation by allosteric activators. Science 339(6124):1216–1219. http://dx.doi.org/10.1126/science.1231097.

[80] Yoshino, J., Conte, C., Fontana, L., Mittendorfer, B., Imai, S., Schechtman, K.B., et al., 2012. Resveratrol supplementation does not improve metabolic function in nonobese women with normal glucose tolerance. Cell Metabolism 16(5):658–664. http://dx.doi.org/10.1016/j.cmet.2012.09.015.

[81] Erion, D.M., Yonemitsu, S., Nie, Y., Nagai, Y., Gillum, M.P., Hsiao, J.J., et al., 2009. SirT1 knockdown in liver decreases basal hepatic glucose production and increases hepatic insulin responsiveness in diabetic rats. Proceedings of the National Academy of Sciences of the United States of America 106(27): 11288–11293. http://dx.doi.org/10.1073/pnas.0812931106.

[82] Rodgers, J.T., Puigserver, P., 2007. Fasting-dependent glucose and lipid metabolic response through hepatic sirtuin 1. Proceedings of the National Academy of Sciences of the United States of America 104(31):12861–12866. http://dx.doi.org/10.1073/pnas.0702509104.

